Journal of
Synchrotron Radiation

ISSN 0909-0495

addenda and errata

MicroGISAXS of Langmuir–Blodgett protein films: effect of temperature on long-range order. Addendum

Eugenia Pechkova,[a,b] Shailesh Tripathi[a,b] and Claudio Nicolini[a,b]*

[a]Nanoworld Institute-CIRSDNNOB, University of Genoa, Corso Europa 30, 16132 Genoa, Italy, and [b]Fondazione ElBA, Piazza SS Apostoli 66, 00187 Rome, Italy. E-mail: manuscript@nwi.unige.it

An extra acknowledgment is published for the paper by Pechkova *et al.* [(2009), *J. Synchrotron Rad.* **16**, 330–335].

The authors of Pechkova *et al.* (2009) would like to add the following acknowledgment: This work was supported by the grant FIRB RBPR05JH2P from MIUR to Claudio Nicolini of University of Genoa.

References

Pechkova, E., Tripathi, S. & Nicolini, C. (2009). *J. Synchrotron Rad.* **16**, 330–335.

 doi:10.1107/S0909049510049344

Journal of
Synchrotron Radiation

ISSN 0909-0495

Received 14 April 2008
Accepted 22 January 2009

MicroGISAXS of Langmuir–Blodgett protein films: effect of temperature on long-range order

Eugenia Pechkova,[a,b] Shailesh Tripathi[a,b] and Claudio Nicolini[a,b]*

[a]Nanoworld Institute-CIRSDNNOB, University of Genoa, Corso Europa 30, 16132 Genoa, Italy, and [b]Fondazione ElBA, Piazza SS Apostoli 66, 00187 Rome, Italy. E-mail: manuscript@nwi.unige.it

The grazing-incidence small-angle X-ray scattering technique has been used here with a microfocus beamline (μGISAXS) to study the effect of temperature on the protein reorganization taking place in a Langmuir–Schaefer multilayered enzyme film. The study appears quite reproducible in the two enzymes being utilized, penicillin G acylase and urease. In-plane and out-of-plane cuts are used to account for the changes in the film thickness and distance between structures taking place by the process of heating up to 423 K and cooling to room-temperature. The out-of-plane cut suggests that the structures are getting closer and are becoming more organized owing to the heating affect. Merging of layers is likely to occur during the heating and cooling process, leading to a loss of correlation between the interfaces of the layers and to the establishment of long-range order. The dramatic increase in long-range order in the Langmuir–Blodgett multilayered enzyme films after heating and cooling, made here apparent by grazing-incidence small-angle X-ray scattering using a microbeam, could in the future open the way to avoiding the bottleneck of protein crystallization for protein structure determination.

Keywords: penicillin G acylase; microGISAXS; urease; LB films.

1. Introduction

Microbeam grazing-incidence small-angle X-ray scattering (μGISAX) is a powerful technique for investigating locally thin films and surfaces (Müller-Buschbaum *et al.*, 2003; Roth *et al.*, 2003; Pechkova *et al.*, 2005; Nicolini & Pechkova, 2006*a*), giving access to length scales of up to several hundred nanometres. The unique combination of a micrometre-sized beam and the reflection geometry allows us to gain, in principle, two orders of magnitude in spatial resolution compared with conventional GISAXS experiments, and thereby represents a very promising tool for studying biomolecular ordered systems, such as Langmuir–Blodgett (LB) thin protein films and crystals (Pechkova &Nicolini, 2003; Pechkova *et al.*, 2005; Nicolini & Pechkova, 2006*a*). It was shown that the LB method, consisting of the formation and proper compression of protein monolayers at the air–water interface (Nicolini *et al.*, 1993), appears capable of depositing the resulting protein monolayers onto solid substrates and to preserve protein structure and function, providing new useful properties such as protein temporal stability, film anisotropy and protein heat stability (Nicolini, 1997; Nicolini & Pechkova, 2006*b*). The secondary structure of all studied proteins in LB films is heat-proofed up to 473 K (for a review, see Nicolini, 1997; Nicolini & Pechkova, 2006*b*). A coherent explanation for the origin and the molecular mechanisms of the protein heat proof in LB films can be drawn by the comparative atomic structure characterization of thermophilic *versus* mesophilic proteins by X-ray crystallographic diffraction and nanogravimetric analysis in protein solution, thin films and crystals, recently pointing to the role of inner bound water in determining protein thermostability (Pechkova, Sivozhelezov & Nicolini, 2007, and references within).

Moreover, it was shown for LB films of photosynthetic reaction centres that special thermal treatment can improve the film ordering (Facci *et al.*, 1994). In order to further understand this phenomenon, it is necessary to study the changes taking place in the protein orientation and long-range order in thin films after heating. Though non-contact 'tapping' mode atomic force microscopy can be used as a topography-sensitive method to provide the surface image of a LB protein sample (Sartore *et al.*, 2000), scattering analysis can give better in-depth insight. Since the original synchrotron study on a heat-proof LB monolayer (Erokhin *et al.*, 1998), much progress in X-ray scattering techniques has been made, namely at the ID13 beamline at the European Synchrotron Radiation Facility (ESRF) in Grenoble (Riekel, 2000) where the μGISAX set-up has been developed (Müller-Buschbaum *et al.*, 2003; Roth *et al.*, 2003). Now it is possible to investigate laterally inhomogeneous surfaces and interfaces with a two order-of-magnitude increase in spatial resolution compared with standard reflection set-ups and a

tenfold lower q_{min} compared with transmission geometry. Using this powerful instrument, in this report we were finally able to study closely the phenomenon of the increased order of the protein LB film after thermal treatment. For this investigation we chose two classical proteins, namely urease, used for the first time by Langmuir and Schaefer for the protein monolayer formation and characterization (Langmuir & Schaefer, 1938), and penicillin G acylase, recently optimally immobilized (Pastorino *et al.*, 2002*a*,*b*). In contrast to previous attempts with the long-range goal to probe the crystal-like structure of protein LB film, we used a very high number of protein monolayers exploiting the possibility of μGISAXS to study the structures embedded in the films as well as the morphology and distribution of the structures in the film.

A three-dimensional highly ordered arrangement of structures in the film can play an important role in the protein nano-template-based crystallization process (Pechkova & Nicolini, 2004), or could even help to avoid the bottleneck of protein crystallization in protein structure determination at the atomic level with the recent progress in X-ray micro- and nanodiffraction techniques (C. Riekel, private communication).

2. Material and methods

2.1. Langmuir–Schaefer protein thin film preparation

Urease was purchased from Sigma and penicillin G acylase (PGA) has been obtained from Antibioticos (Pastorino *et al.*, 2002*a*,*b*). These two enzyme thin films were prepared at the air–water interface utilizing a Langmuir trough, with a subphase volume of 800 ml and a surface area of 44 × 11 cm. The surface pressure was measured to be 20 mN m^{-1} by means of a Willhelmy balance. The procedures adopted to form protein films of urease were as described by Langmuir & Schaefer (1938) and Nicolini (1997), while for PGA the thin films were prepared by the 'protective plate' method (Troitsky *et al.*, 1996; Pastorino *et al.*, 2002*a*,*b*).

The Langmuir–Schaefer modification of the LB technique (horizontal lift) was used and the floating monolayer is transferred over the substrate surface by horizontally touching the monolayer and the layer transfers onto the substrate. In such a way the 60 monolayers were subsequently deposited one over another using a silica wafer as the substrate. Atomic force microscopy (AFM) characterization (shown in Fig. 1 for PGA and in Fig. 2 for urease) and the routine assays discussed and referenced above (Nicolini, 1997; Pastorino *et al.*, 2002*a*,*b*;

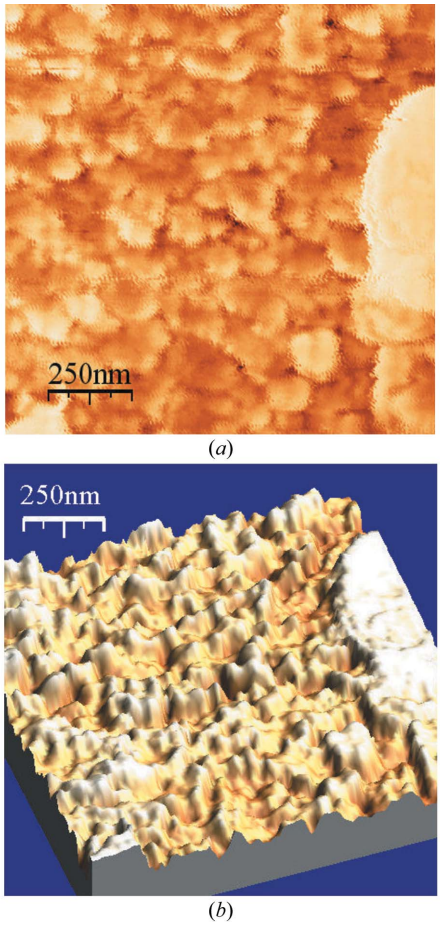

Figure 1
Representative AFM image of PGA (LB film of 60 monolayers) at room temperature in two dimensions (*a*) and three dimensions (*b*). The vertical range (*z*) goes up to 60 nm.

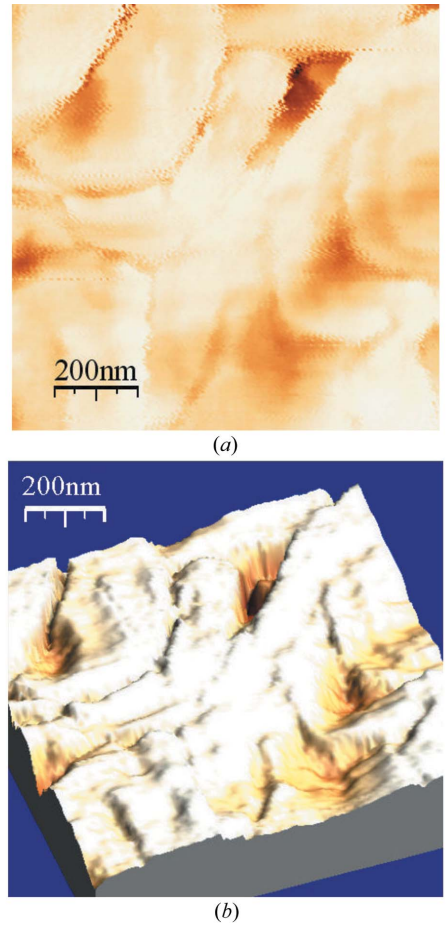

Figure 2
Representative AFM image of urease (LB film of 60 monolayers) at room temperature in two dimensions (*a*) and three dimensions (*b*). The vertical range (*z*) goes up to 200 nm.

Nicolini & Pechkova, 2006*b*), namely Brewster microscopy, isotherms, absorbance, transmission infrared spectroscopy and nanogravimetry *versus* number of layers, confirm the accurate LB film formation as indicated up to exactly 60 monolayers (not shown).

Each silica wafer, of dimensions 5 × 5 mm, was properly cleaned by sulfuric acid solution and dried before thin film deposition. Each deposited monolayer was dried by nitrogen flux. The fresh film for each enzyme was divided into two sample groups: the first group was incubated at 293 K, while the second group was placed in an oven pre-heated up to 423 K for 10 min, and then cooled down to room temperature.

2.2. Atomic force microscopy

Images of the protein thin LB films have been obtained in tapping mode with a cantilever I type NSC14/Cr-Au Mikro-Mash in a dry atmosphere utilizing an instrument based on the SPMagic controller built in-house (Sartore *et al.*, 2000; Pechkova, Sartore *et al.*, 2007). The freeware *WSxM* (http://www.nanotec.es/) was used to process the acquired images. The typical resonance frequency of the cantilever tip is between 110 and 220 kHz, and the proper positioning of the cantilever on the AFM tip holder has been found at a frequency of 92 kHz, with intensity 0.6 V. The set point for loop control was at 0.2 V. The integral gain value during image grabbing was set at 4.4 (I gain) and the proportional gain value during image acquisition was set at 8.03 (P gain). Figs. 1 and 2 show AFM images of the superposed 60 layers of PGA and urease protein at room temperature, both in two-dimensional and in three-dimensional arrangement for PGA (Fig. 1) and urease (Fig. 2), indicating an ordered protein organization quite distinct in enzyme size and overall morphology.

2.3. MicroGISAXS experiments

MicroGISAXS experiments were performed at the ID13 microfocus beamline of ESRF, Grenoble, France (Riekel, 2000). The wavelength of the monochromatic beam was λ = 0.9755 Å. The beam size obtained after focusing by crossed Fresnel lenses was 10 × 10 µm. As shown in Fig. 3 and described in detail by Roth *et al.* (2003) and Pechkova *et al.* (2005), the direct beam was blocked by a beam stop of diameter 300 µm and the specular beam located at $\alpha_f = \alpha_i$ (α_i is the incidence angle and α_f the exit angle) was stopped by a square lead beamstop of 4 mm edge length. The sample was mounted on an *xyz*-translation stage, and a two-dimensional goniometer (α, ψ) allowed adjustment of the sample orientation (Fig. 3 and Roth *et al.*, 2003). Owing to the fixed incident angle of about 1°, the beam footprint is enlarged in the *x* direction, leading to an actual beam size of about 300 µm × 5 µm ($x \times y$). The basic experimental set-up for thin film study using this µGISAXS (Roth *et al.*, 2003; Pechkova *et al.*, 2005) is shown in Fig. 3. The size S of the beam in grazing-incidence geometry is given as $S = X_v/\tan(\alpha_f)$, where α_f is the angle of incidence of the beam in the sample and X_v is the vertical beam size.

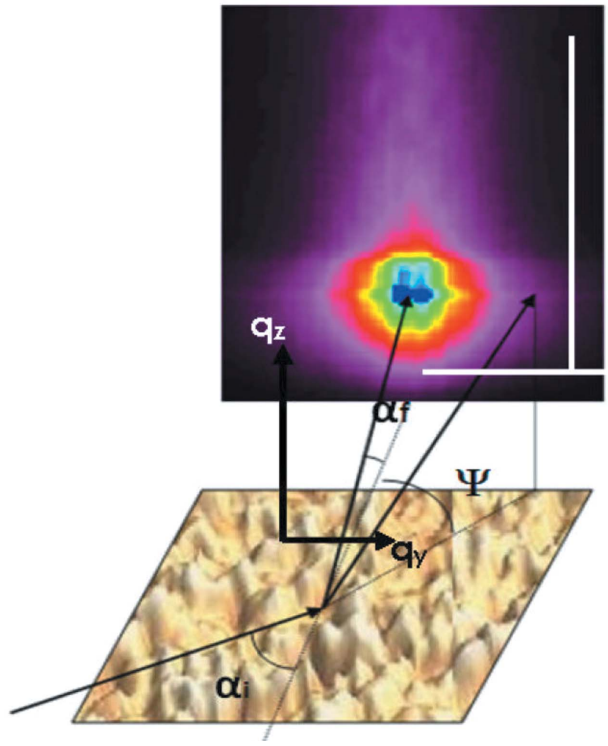

Figure 3
Representation of the principle of µGISAXS measurement. In this case the surface is the protein thin LB film. α_i is the incidence angle and α_f the exit angle. Scattered beams are collected in both directions, *i.e.* in planes Ψ and α, which correspond to axes q_y and q_z of the reciprocal space, where q_z is the wavevector component perpendicular to the surface and q_y is the wavevector component parallel to the surface. A characteristic feature of a GISAXS pattern is the Yoneda peak (Yoneda, 1963), shown here in blue.

The scattering data were recorded using a two-dimensional charge-coupled detector (MAR CCD) with 2048 × 2048 pixels of size 64.45 µm × 64.45 µm and 16-bit readout. The sample-to-detector distance was calibrated to be 945.7 mm by an Ag-behenate standard (Blanton *et al.*, 1995). A two-dimensional detector scan of 2048 × 2048 pixels was used to calculate the scattered intensity at a fixed angle of incidence α_i of the X-ray beam. A two-dimensional scattering profile was obtained, which is an arrangement of a horizontal profile at fixed α_f and a vertical profile at fixed Ψ. This includes the resonant diffused scattering and Yoneda (Yoneda, 1963) peaks.

2.4. MicroGISAXS data analysis

Scattering in reciprocal space q_y and q_z is shown in Fig. 3. Here, q_y and q_z denote the wavevector components parallel and perpendicular to the surface, respectively. In order to analyze the data, two different cuts can be performed, *i.e.* out-of-plane cuts and detector cuts. The out-of-plane cut is a cut at fixed q_z and the detector cut is at fixed q_y.

Here,

$$q_x = 2\pi(\cos\Psi\cos\alpha_f - \cos\alpha_i)\lambda, \qquad (1)$$

$$q_y = 2\pi/\lambda(\sin\Psi\cos\alpha_f), \quad (2)$$

$$q_z = 2\pi/\lambda(\sin\alpha_i + \sin\alpha_f). \quad (3)$$

A detector cut reveals information about the structures vertical to the sample surface, while an out-of-plane cut reveals information about the distribution of structures along the film. Thus off-specular intensity gives information about the distance between isolated structures in the film and their shape (Naudon & Thiaudiere, 1996). These cuts are performed using the software *FIT2D*. Output files from this software are used for graphical representations.

A characteristic feature of a μGISAXS pattern is the Yoneda peak (Yoneda, 1963; Pechkova & Nicolini, 2006; Nicolini & Pechkova, 2006*a*). This peak occurs at angles α_i, $\alpha_f = \alpha_c$, where α_c is the critical angle of the sample. The critical angle depends on the material *via* the real part of the refractive index, and hence on the density and roughness of the layer. The relative intensities of two or more Yoneda peaks can hence be interpreted in terms of film reorganization related to the build up of layers, islands or holes.

3. Results and discussions

From the AFM analysis (Figs. 1 and 2) the clear difference in the size and morphology of protein aggregates for two proteins can be observed. In the case of urease, its aggregate in the AFM images (Figs. 2*a* and 2*b*) is larger than for PGA (Figs. 1*a* and 1*b*), owing to its larger molecular weight. At 423 K (Fig. 1) the PGA LB films appear better organized in both the two-dimensional and three-dimensional space than at 293 K (not shown), confirming previous scanning tunneling microscopy (STM) analysis of the photosynthetic reaction centre (Facci *et al.*, 1994). However, from the systematic AFM analysis of treated and untreated samples of both enzymes it becomes clear that with this technique it is difficult to quantify the large differences in the LB structure re-organization. Moreover, only the last single layer of the LB protein film can be analyzed, and no information about internal structural re-arrangement can be obtained.

Instead, with the present X-ray scattering analysis, two different μGISAXS patterns are clearly distinguishable in the case of both urease (Figs. 4*a* and 4*b*) and PGA (Fig. 4*c* and 4*d*) LB films for heat-treated *versus* untreated samples, with uniquely reproducible out-of-plane (Figs. 5 and 6) and detector (Fig. 7) scans in the case of both enzymes. For urease, Fig. 4(*b*) shows the typical spectra from samples incubated at room temperature, while Fig. 4(*a*) shows the scattering from a sample which was heated up to 423 K and cooled down to room temperature. In this two-dimensional map, Yoneda peaks are observed. It is evident that the sample which has undergone the heating treatment gives the two peaks in the Yoneda region. They are also clearly seen on the intensity plot of a horizontal slice of the μGISAXS images indicated in Fig. 4. Fig. 5 shows the intensity profiles obtained after performing out-of-plane cuts in the Yoneda region with respect to the q_y pixels. Only structures parallel to the surface are probed

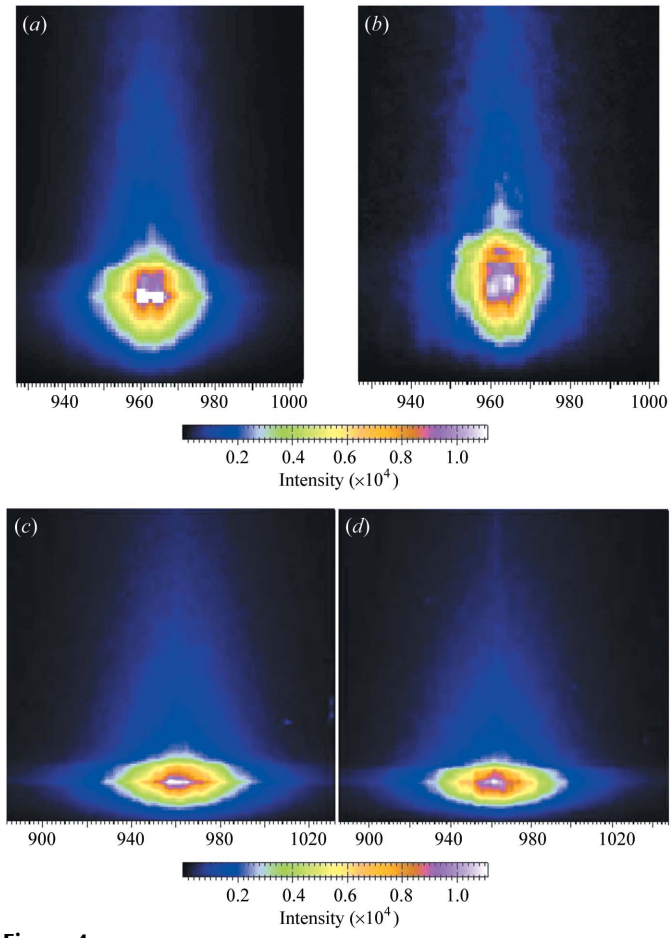

Figure 4
GISAXS images obtained of 60 monolayers of urease film heated up to 423 K and subsequently cooled down to room temperature (*a*) and incubated at 293 K (*b*), and of PGA film heated up to 423 K and subsequently cooled to room temperature (*c*) and incubated at 293 K (*d*). The intensity scale is given for each image.

through this cut. In Fig. 5(*a*) the profiles for urease thin film either heated up to 423 K or incubated at 293 K *versus* pixels are shown. It can be seen that the first profile has two clear symmetrical peaks, while the latter appears smoother. In the case of PGA LB films, the μGISAXS patterns are also different for treated and untreated samples, indicating a long-range order induced by heat treatment. From Figs. 4(*c*) and 4(*d*) the differences in the Yoneda region can be observed, while the out-of-plane scans in the Yoneda region of the two-dimensional μGISAXS scattering profiles of heat-treated and untreated samples of the same PGA are compared in Fig. 5(*b*). The PGA LB film heated up to 423 K gives a more symmetric profile than the film incubated at 293 K. Moreover, there are more peaks and they are more pronounced than in the untreated sample profile, which is likely due to an increase in the long-range order of the film.

Fig. 6 shows the double logarithmic curve of the intensity in reciprocal space, *i.e. versus* q_y. The clear difference between the curve corresponding to the LB protein film stored at room temperature and those heated up to 423 K and consequently cooled can be observed both in the case of PGA (Fig. 6*a*) and urease (Fig. 6*b*). These curves take into account the form

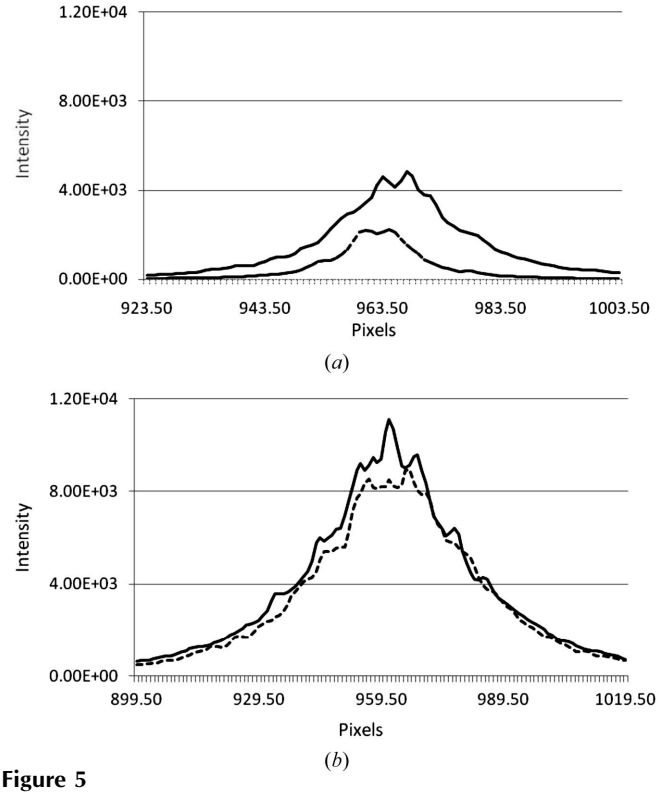

Figure 5
Out-of-plane scan in the Yoneda region of the two-dimensional μGISAXS scattering profiles. Intensity plot on performing a horizontal slice of the GISAXS images for urease (*a*) and PGA (*b*) at 423 K (full line) and 293 K (dashed line) *versus* pixels.

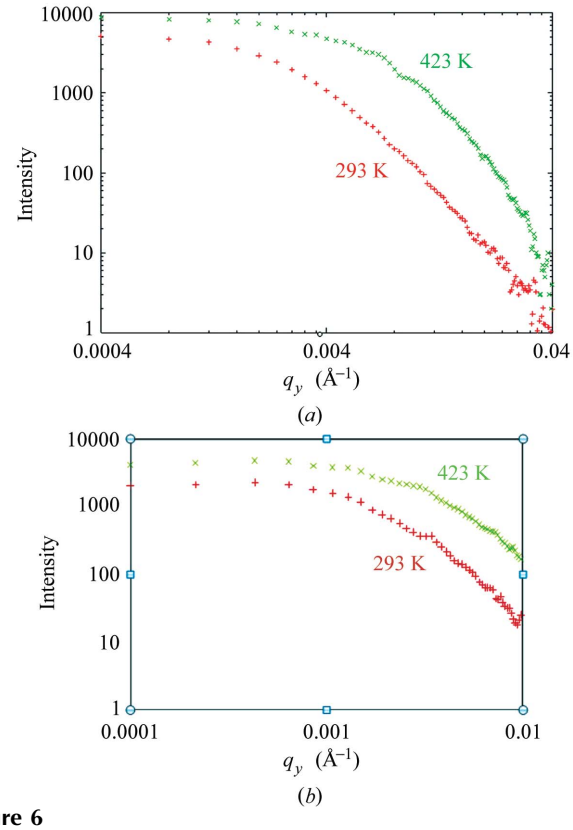

Figure 6
Intensity *versus* q_y plot on a logarithmic scale of 293 K (+) and 423 K (×) PGA LB films (*a*) and urease LB films (*b*).

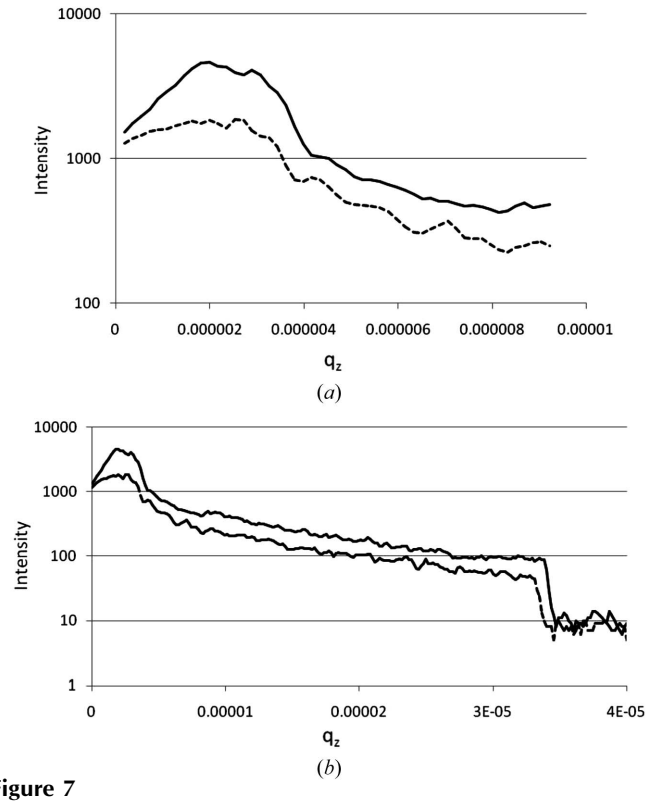

Figure 7
Detector scan, *i.e.* intensity (*I*) *versus* q_z in the Yoneda region (*a*) and *versus* q_z within and outside the Yoneda region (*b*), both for urease film at 423 K (full line) and at 293 K (dashed line).

factor and structure factor of the structures in the film, pointing quite clearly to a more pronounced long-range order in the heated sample. If the objects have well defined geometry, the structure factor yields the most prominent in-plane length scale ξ. The peak in both cases corresponds to ordered structures present in the film. In this case the occurrence of maxima along q_y in Figs. 6(*a*) and 6(*b*) allows the determination of the most prominent length scale ξ (Pechkova *et al.*, 2005),

$$\xi \simeq 2\pi/q_y. \tag{4}$$

Namely, from the data in Fig. 6, the most prominent in-plane length can be calculated and compared for the cases of structures in PGA films at two different temperatures. In the case of PGA LB film stored at 293 K the in-plane length is of the order of 210 ± 30 nm. For the PGA LB film which has undergone the heating and cooling processes, this is of the order of 158 ± 19 nm. Thus a decrease in the in-plane length scale is clearly visible in this case.

In order to study the LB film structure perpendicular to the surface, a detector scan was performed by making a vertical cut at $q_y = 0$. This cut shows the locally ordered films along the vertical direction. Different interfaces scatter the X-rays individually leading to interaction of the scattered rays. If the interfaces are correlated then interference leads to resonance diffused scattering, while in the opposite case (interfaces are not correlated) individual scatterings superpose (Müller-Buschbaum & Stamm, 1998). This correlation could occur in

the case of protein multilayers as the roughness correlation between interfaces of different layers. The partial phase coherence of the waves scattered from the interfaces concentrates the intensity in narrow sheets. These sheets of resonant diffused scattering are parallel to q_x and at the centre satisfy the Bragg condition $\Delta q_z = 2\pi/d_{\rm corr}$.

In conclusion, from the detector cut along the vertical q_z cut at $q_y = 0$ shown in Fig. 7, more Yoneda peaks are apparent in the heated than in the unheated urease LB film, pointing to a significant reorganization of ureases in the multilayers LB film associated with heating up to 423 K and cooling.

4. Conclusions

LB films of different proteins, such as immunoglobuline, thioredoxin, cytochrome P450 and bacteriorhodopsin, were studied by synchrotron X-ray scattering (Erokhin *et al.*, 1998), showing that thermal treatment of the films results in a pronounced increase of the film order. Bragg reflections, which indicate the ordering in the direction perpendicular to the film plane, were indeed recorded for films after thermal treatment for all the proteins investigated, compatibly with the STM studies of heated LB photosynthetic reaction centres (Facci *et al.*, 1994). Conversely, the ordering of the films prepared without thermal treatment appears rather poor. The present μGISAX study of protein LB multilayers film supports these previous synchrotron radiation (Erokhin *et al.*, 1998) and STM (Facci *et al.*, 1994) studies and confirms that heating the protein LB film and subsequently cooling down leads to a quite more ordered arrangement. Moreover, the μGISAX method appears to yield new insights on the long-range order previously unforeseeable and on the type of reorganization taking place within the LB multilayers. We thereby suggest one of the possible models for reorganization of the structures in the film (Fig. 8), in terms of a higher packing occurring when the film is subjected to high temperature and subsequently cooled down. As shown by μGISAXS, the in-plane structure distance is indeed decreasing with heat compatibly with the merging of layers of macromolecular structures, with the decrease in the plane length being likely due to the loss of water caused by LB formation and heating to 423 K. However, considering the qualitative nature of the analysis here provided of the obtained μGISAXS data, this hypothesis needs further quantitative study in order to be confirmed.

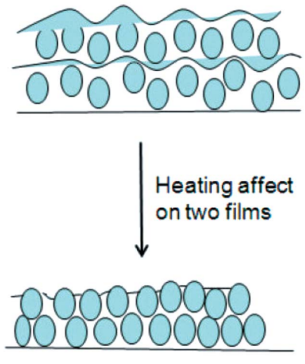

Figure 8
Scheme of one of the possible physical interpretations for the phenomenon of decreasing of film thickness and its re-ordering upon heating up to 423 K and cooling to room temperature. The increasing of structural correlation between two protein monolayers as a consequence of heating and cooling is shown.

This project was supported by grants to Fondazione ElBA by MUR (Ministero Università e Ricerca) for 'Funzionamento' and for Biocatalysis and by a FIRB International Grant on Proteomics and Cell Cycle (RBIN04RXHS) from MUR to CIRSDNNOB-Nanoworld Institute of the University of Genova.

References

Blanton, T. N., Huang, T. C., Toraya, H., Hubbard, C. R., Robie, S. B., Louer, D., Gobel, H. E., Will, G., Gilles, R. & Raftery, T. (1995). *Powder Diffr.* **10**, 91–95.
Erokhin, V., Carrara, S., Guerzoni, S., Ghibellini, P. & Nicolini, C. (1998). *Thin Solid Films*, **327–329**, 636–638.
Facci, P., Erokhin, V. & Nicolini, C. (1994). *Thin Solid Films*, **243**, 403–406.
Langmuir, I. & Schaefer, V. J. (1938). *J. Am. Chem. Soc.* **60**, 1351–1360.
Müller-Buschbaum, P., Roth, S. V., Burghammer, M., Diethert, A., Panagiotou, P. & Riekel, C. (2003). *Europhys. Lett.* **61**, 39–645.
Müller-Buschbaum, P. & Stamm, M. (1998). *Macromolecules*, **31**, 3686–3692.
Naudon, A. & Thiaudiere, D. (1996). *Surf. Coat. Technol.* **79**, 103–107.
Nicolini, C. (1997). *Trends Biotechnol.* **15**, 395–401.
Nicolini, C., Erokhin, V., Antolini, F., Catasti, P. & Facci, P. (1993). *Biochim. Biophys. Acta*, **1158**, 273–278.
Nicolini, C. & Pechkova, E. (2006*a*). *J. Cell. Biochem.* **97**, 544–552.
Nicolini, C. & Pechkova, E. (2006*b*). *J. Nanosci. Nanotechnol.* **6**, 2209–2236.
Pastorino, L., Berzina, T. S., Troitsky, V. I., Bernasconi, E. & Nicolini, C. (2002*a*). *Colloids Surf. B*, **23**, 289–293.
Pastorino, L., Berzina, T. S., Troitsky, V. I., Fontana, M. P., Bernasconi, E. & Nicolini, C. (2002*b*). *Colloids Surf. B*, **23**, 357–363.
Pechkova, E. & Nicolini, C. (2003). *Proteomics and Nanocrystallography*. New York: Kluwer.
Pechkova, E. & Nicolini, C. (2004). *Trends Biotechnol.* **22**, 599–602.
Pechkova, E. & Nicolini, C. (2006). *J. Cell. Biochem.* **97**, 553–560.
Pechkova, E., Roth, S. V., Burghammer, M., Fontani, D., Riekel, C. & Nicolini, C. (2005). *J. Synchrotron Rad.* **12**, 713–716.
Pechkova, E., Sartore, M., Giacomelli, L. & Nicolini, C. (2007). *Rev. Sci. Instrum.* **78**, 093704.
Pechkova, E., Sivozhelezov, V. & Nicolini, C. (2007). *Archiv. Biochem. Biophys.* **466**, 40–48.
Riekel, C. (2000). *Rep. Prog. Phys.* **63**, 233–262.
Roth, S. V., Burghammer, M., Riekel, C., Muller-Bushbaum, P., Diethert, A., Panagiotou, P. & Walter, H. (2003). *Appl. Phys. Lett.* **82**, 1935–1937.
Sartore, M., Pace, R., Faraci, P., Nardelli, D., Adami, M., Ram, M. K. & Nicolini, C. (2000). *Rev. Sci. Instrum.* **71**, 2409–2413.
Troitsky, V. I., Sartore, M., Berzina, T. S., Nardelli, D. & Nicolini, C. (1996). *Rev. Sci. Instrum.* **67**, 4216–4223.
Yoneda, Y. (1963). *Phys. Rev.* **131**, 2010–2013.